

DTIC FILE COPY

AD-A216 245



DTIC  
ELECTE  
JAN 02 1990  
S B D

DEVELOPMENT OF AN ALTERNATIVE  
CONCENTRATION PROBE  
CALIBRATION METHOD

THESIS

George Rudolph Stoller, Jr.  
Captain, USAF

AFIT/GAE/ENY/89D-37

DEPARTMENT OF THE AIR FORCE  
AIR UNIVERSITY

**AIR FORCE INSTITUTE OF TECHNOLOGY**

Wright-Patterson Air Force Base, Ohio

**DISTRIBUTION STATEMENT A**

Approved for public release;  
Distribution Unlimited

89 12 29 048

AFIT/GAE/ENY/89D-37

DEVELOPMENT OF AN ALTERNATIVE  
CONCENTRATION PROBE  
CALIBRATION METHOD

THESIS

Presented to the Faculty of the School of Engineering  
of the Air Force Institute of Technology  
Air University  
In Partial Fulfillment of the  
Requirements for the Degree of  
Master of Science in Aeronautical Engineering

George Rudolph Stoller, Jr., B.S.  
Captain, USAF

December, 1989

Approved for public release; distribution unlimited

### Acknowledgments

I am sure that a multitude of thanks have been offered over the years at AFIT, but certainly none are as sweet as those uttered by each departing class. I desire then, to add my voice to the echoes of those that have come before me.

First and foremost, I would like to thank my Heavenly Father, who graciously granted me strength to make it through this training.

I would like to thank my "academic father," Dr William Elrod, for his confidence in my work and his uncanny ability to see the problem and fix it. In that same vein, I wish to express gratitude to my "academic older brother," Capt Fred Tanis, whose support was certainly the linchpin of my study. Thanks also to my committee members, Dr M.E. Franke and Capt Jim Planeaux, for their thoughtful consideration of my work.

Many thanks go to the laboratory personnel, in particular Mark Derriso and Andy Pitts, two gentlemen that took a special interest in what I was doing. When Mark and Andy made a contribution to the project, I was confident that they would personally make sure the job was completed well.

My gratitude goes to John Brohas and the rest of the shop crew. John was an invaluable source of insight and experience. His work was top-notch.

Finally, I wish to express the deepest of thanks to my family and friends, especially the close friends I have made in Dayton, whom I consider to be my extended family. I have been blessed with a bulwark of friendships, to which I thankfully clung during many dark and stormy trials.

George Rudolph Stoller, Jr.

Accession For	
NTIS GRA&I	<input checked="checked" type="checkbox"/>
DTIC TAB	<input type="checkbox"/>
Unannounced	<input type="checkbox"/>
Justification	
By	
Distribution/	
Availability Codes	
Dist	Avail and/or Special
A-1	



## *Table of Contents*

	Page
Acknowledgments . . . . .	ii
Table of Contents . . . . .	iii
List of Figures . . . . .	v
List of Symbols . . . . .	vi
Abstract . . . . .	viii
I. Introduction . . . . .	1-1
1.1 Background . . . . .	1-1
1.2 Objectives and Scope . . . . .	1-2
1.3 Sequence of Presentation . . . . .	1-2
II. Theory of Probe Operation . . . . .	2-1
III. Experimental Apparatus . . . . .	3-1
3.1 Mixture Supply System . . . . .	3-1
3.1.1 Constituent Metering Subsystem . . . . .	3-1
3.1.2 Constituent Mixing Subsystem . . . . .	3-3
3.2 Steady Flow Test System . . . . .	3-3
3.3 Tank Discharge Test System . . . . .	3-4
3.4 Hot Wire Anemometer System . . . . .	3-5
3.5 Concentration Probe . . . . .	3-5
3.6 Data Acquisition System . . . . .	3-6

	Page
IV. Experimental Procedures . . . . .	4-1
4.1 General Procedures . . . . .	4-1
4.1.1 Venturi Calibration . . . . .	4-1
4.1.2 Hot Wire Anemometer Preparation . . . . .	4-1
4.1.3 Start-up . . . . .	4-1
4.2 Steady Flow Probe Calibration Procedure . . . . .	4-2
4.3 Tank Discharge Probe Calibration Procedure . . . . .	4-2
V. Results . . . . .	5-1
5.1 Steady Flow Calibration Method Results . . . . .	5-1
5.2 Tank Discharge Method Results . . . . .	5-2
5.3 Comparison of Steady Flow and Tank Discharge Results . . .	5-6
VI. Conclusions and Recommendations . . . . .	6-1
6.1 Conclusions . . . . .	6-1
6.2 Recommendations . . . . .	6-1
Appendix A. Properties of Mixtures . . . . .	A-1
Appendix B. Venturi Calibration . . . . .	B-1
Bibliography . . . . .	BIB-1
Vita . . . . .	VITA-1

## *List of Figures*

Figure	Page
2.1. Basic design of a supersonic aspirating concentration probe . . . . .	2-2
3.1. Schematic of mixture supply and steady flow test systems . . . . .	3-2
3.2. Constituent mixing device for helium and air streams . . . . .	3-4
3.3. Tank discharge schematic . . . . .	3-5
3.4. Basic concentration probe . . . . .	3-6
5.1. Steady flow calibration curve . . . . .	5-3
5.2. Steady flow curves with different sensor $P_0$ values . . . . .	5-3
5.3. Reynolds versus Nusselt numbers from tank discharge data . . . . .	5-4
5.4. Tank discharge method: sensor heat loss correlation . . . . .	5-5
5.5. Comparison of one sample interval, steady flow vs. discharge method .	5-6
5.6. Calibration method comparison: steady flow vs. tank discharge . . . .	5-8
5.7. Calibration method comparison and King's law . . . . .	5-8
A.1. Mixture viscosity as a function of helium molar fraction . . . . .	A-1
A.2. Mixture thermal conductivity as a function of helium molar fraction . .	A-2
A.3. Mixture specific heat as a function of helium molar fraction . . . . .	A-2
A.4. Mixture Prandtl number as a function of helium molar fraction . . . . .	A-3

# *List of Symbols*

Symbol	Definition
<i>Alphanumeric Symbols</i>	
$a$	venturi throat area
$A_{ch}$	sensor channel cross sectional area
$A_{cyl}$	surface area of the cylinder
$C_d$	discharge coefficient
$d$	diameter of the hot wire
$d_v$	venturi throat diameter
$D$	venturi inlet diameter
$Gr$	Grashof number
$h$	heat transfer coefficient of the sensor
$I$	current
$k_f$	thermal conductivity of the fluid
$K$	Knudsen number
$\dot{m}_{mix}$	mixture mass flow rate
$\dot{m}_{sn}$	mass flow rate through choked nozzle
$M$	species molecular weight
$Nu_d$	Nusselt number
$P_0$	sensor chamber total pressure
$Pr$	Prandtl number
$Q$	heat transferred to the fluid
$R_s$	sensor resistance at its operating temperature
$R_{ser}$	bridge circuit series resistance
$Re_d$	Reynolds number
$T_0$	sensor chamber total temperature
$T_m$	mean film temperature
$T_s$	sensor operating temperature
$T_\infty$	fluid temperature

# Symbol

# Definition

$V_{br}$	bridge supply voltage
$x_{He}$	molar fraction of helium
$Y$	Tanis correlation ordinate
$Y_r$	compressible fluid expansion ratio

## *Greek Symbols*

$\beta$	ratio of venturi throat to inlet diameter
$\Delta p$	pressure drop between inlet and throat
$\mu_f$	viscosity of the fluid
$\rho_1$	upstream fluid density, $\rho_1 = p_1/RT_1$



*Abstract*

Aspirating, hot wire concentration probes are used to measure point-wise binary species concentrations in supersonic gaseous flow fields. Calibration of such probes is usually carried out by exposing the probe to a known mixture as it discharges from a fixed volume (or tank.) A new, steady flow method for the calibration of helium/air concentration probes has been developed and has been compared with an existing tank discharge method. The two calibration curves have been found to be in close agreement, with a difference of 0.05 helium molar fraction between them for given a value of wire heat loss. Probe design is suspected of being responsible for this slight variation in helium molar fraction. Hence, either method can be used for calibration of such probes.

# DEVELOPMENT OF AN ALTERNATIVE CONCENTRATION PROBE CALIBRATION METHOD

## *I. Introduction*

The study of supersonic shear flows has been gathering momentum in recent times, spurred onward by keen interest in supersonic and hypersonic combustion processes. It is very likely that important information can be gained if, for instance, two shearing streams are modelled by different gases, like helium and air. Data on the local molar concentration of the constituents would give useful information on the mixing occurring in the shear layer. The aspirating, hot wire concentration probe is a logical choice for the application. By isolating the effect that fluid composition has on wire heat loss from the other effects of mass velocity and temperature difference, the probe is able to sense changes in concentration. The sensor is of no use, however, unless it is calibrated.

### *1.1 Background*

Calibration of aspirating concentration probes has generally been accomplished by exposing the probe to a batch mixture of known concentration. The constituent gases are combined in a tank and the probe is then exposed to the known mixture as it discharges from the tank. This method was employed by Brown and Rebollo (3:650) using a 500 cubic in. volume. The volume was pressurized to 105 psia and bled slowly down to 0.5 psia, with probe measurements taken at various pressures. Adler used a similar set up to conduct a parametric study of hot wire concentration measurement (1:166). The most recent group of published investigators, headed by Ng, has also used a discharging pressure vessel to construct a set of calibration curves (9:3). Unlike those before, the probe calibrated in that procedure was designed for use in supersonic shear layers. At the time of this writing, Tanis is also using an aspirating concentration probe in the study of supersonic turbulent shear layer mixing (10). His probe is similarly calibrated using the tank discharge method.

There appears to be no mention of a steady flow calibration method in the literature, therefore this study was conducted to see how such a method might compare with the existing tank discharge method.

### *1.2 Objectives and Scope*

The purpose of this study was to attain the following objectives:

1. Develop a steady flow mixing system for helium/air concentration probe calibration.
2. Use an existing tank discharge calibration system to generate a calibration curve suitable for comparison with the steady flow curve.
3. Compare the resulting calibration curves.
4. Compare the experimentally based calibration curves and the heat loss curve predicted by theory (King's law.)

The system was designed to produce a steady, subsonic flow. Mixture was variable from 100% air to 100% helium. Total pressure at the sensor location (near the enclosed hot wire) was variable from 3 to 5 psia. Fluid total temperature remained essentially constant at ambient (520 R.)

### *1.3 Sequence of Presentation*

Following this chapter, the theory and fundamental operating concept of the probe is presented in Chapter Two. Chapter Three describes the experimental apparatus, followed by Chapter Four which outlines procedures used to collect the data. Results are given in Chapter Five, with the conclusion and recommendation section directly following in Chapter Six.

## II. Theory of Probe Operation

The theory governing operation of the aspirating, hot wire concentration probe follows directly from the fundamentals of hot wire anemometry. A sensing element such as a fine tungsten wire is electrically heated well above the flow temperature. The heat transfer that occurs is characterized by the familiar equation

$$Q = I^2 R_s = h A_{cyl} (T_s - T_\infty), \quad (2.1)$$

where  $Q$  is the heat transferred to the fluid,  $I$  is the current passing through the sensing element,  $R_s$  is the sensor resistance at its operating temperature,  $h$  is the heat transfer coefficient for the sensing element, in this case a circular cylinder in cross flow,  $A_{cyl}$  is the surface area of the cylinder,  $T_s$  is the sensor operating temperature and  $T_\infty$  is the fluid temperature. The temperature profile along the length of the wire is assumed to be flat—this is equivalent to assuming that convection heat loss is much larger than conduction heat loss from the ends. In addition, radiation heat loss is assumed to be negligible (7:64).

A hot wire sensor detects changes in flow variables by sensing changes in wire heat loss,  $Q$ . This heat transfer is a function of four variables related to the fluid: velocity, temperature, pressure and composition (1:163). Isolating the effects of the first three variables from the composition variable makes the wire sensitive to concentration fluctuations only. Isolation of the composition variable is accomplished by enclosing the sensor in a channel and placing an orifice behind it. As an example of this *aspirated* configuration, a very recent design by Ng (9:1) is shown in Figure 2.1. The orifice regulates mass velocity past the sensor, thus causing the velocity variable to be isolated from the composition variable. The pressure behind the orifice is lowered so that it becomes a choked. This is useful because measurement of total temperature and pressure near the sensor can then be used to determine mass flow rate through the choked orifice,  $\dot{m}_{sn}$ , and thus quantify the mass velocity past the sensor via the mass flux,  $\dot{m}_{sn}/A_{ch}$ .  $A_{ch}$  is the area of the channel at the sensor location. Therefore, armed with the knowledge of temperature, pressure and velocity (imbedded in mass flux), the task of forcing concentration to have the dominant effect on wire heat loss is complete.

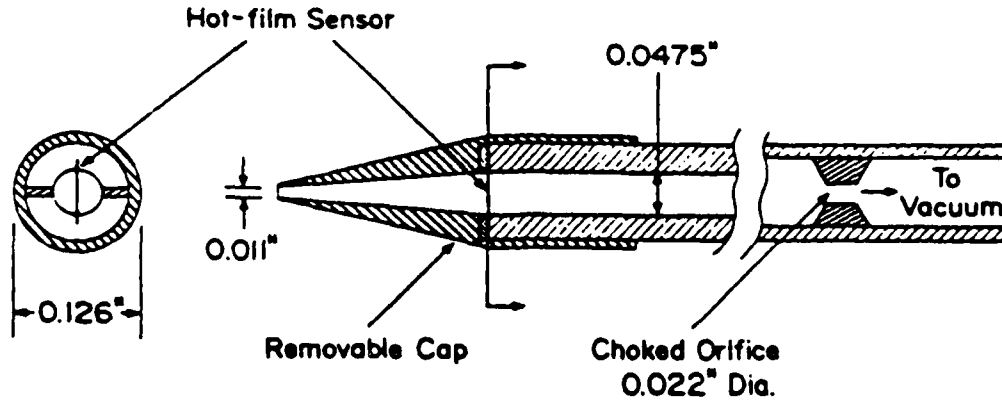


Figure 2.1. Basic design of a supersonic aspirating concentration probe

The implementation of this concept is somewhat more complicated than the preceding description might indicate. The value of  $Q$  in Equation 2.1 is obtained from measurements made with a hot wire anemometer system. In the constant temperature mode, the anemometer system works to keep  $T_s$  at a set operating temperature. If  $T_\infty$  is measured (or assumed to be constant), the temperature difference between the wire and the fluid is fixed. It then appears that  $h$  is the only variable left in Equation 2.1 that can yield information on concentration. Dimensional analysis of forced convection parameters led to the development of the Nusselt number,  $Nu$ , a non-dimensional quantity that incorporates  $h$ .  $Nu$  is commonly expressed as

$$Nu_d = \frac{hd}{k_f} \quad (2.2)$$

The diameter of the hot wire,  $d$ , is the characteristic length. The thermal conductivity of the fluid,  $k_f$ , is evaluated at the mean film temperature,  $T_m$ , determined from the expression

$$T_m = \frac{T_s + T_\infty}{2} \quad (2.3)$$

Solving for  $h$  in Equation 2.2 and then substituting it into Equation 2.1 yields

$$\frac{Q}{\pi l k_f (T_s - T_\infty)} = Nu_d \quad (2.4)$$

Many heat transfer laws involving  $Nu_d$  have been proposed over the years, most of them developed assuming cylinders of infinite length (5:62) but adaptable for use with hot wire anemometers. In general,  $Nu_d$  can be expressed as

$$Nu_d = Nu_d(Re, Gr, Pr, K, T_m/T_\infty) \quad (2.5)$$

Reynolds number,  $Re = \rho V x / \mu_f$ , is usually expressed as  $Re_d$ , with the characteristic length given by the diameter of the hot wire,  $d$ . Since free and forced convection are normally treated separately,  $Gr$ , the Grashof number, is dispensed with (5:358). In practice, the Knudsen number,  $K$ , is not included as a parameter explicitly. Collis and Williams found the effect of *temperature loading*,  $T_m/T_\infty$ , to be an important factor in their experiments with hot wires in pure air (5:369), which led to their version of the heat transfer law for an infinite cylinder:

$$Nu_d \left( \frac{T_m}{T_\infty} \right)^{-0.17} = 0.24 + 0.56 Re_d^{0.45} \quad (2.6)$$

for  $0.02 < Re_d < 44$ . (Prandtl number was not included in this correlation since it did not vary appreciably with temperature for pure air (5:358).) Equation 2.6 was obtained experimentally, but it resembles the often-cited King's law, which can be expressed as

$$Nu_d = \frac{1}{\pi} + \left( \frac{2}{\pi} Re_d Pr \right)^{0.5} \quad (2.7)$$

where the Prandtl number,  $Pr = \mu c_p / k_f$ , is included. Thus, King's law is of the general form

$$Nu_d = Nu_d(Re_d, Pr) \quad (2.8)$$

A comparison of Equation 2.6 with Equation 2.7 shows that both equations include Reynolds number, but the Collis and Williams equation lacks the information on fluid properties ( $k, c_p$ ) inherent in  $Pr$ , while King's equation does not take into account the effects of  $T_m/T_\infty$ . Equation 2.7 was derived by King on the basis of potential flow around a wire, and has been shown experimentally to overestimate the heat transfer by as much as 40% (5:361). Nevertheless, Adler used Equation 2.7 as a model suitable for comparison

with his experimental concentration probe data (1:164). An examination of Equation 2.7 reveals that all the flow variables affecting sensor response are at least rudimentally represented: velocity, temperature and pressure in the mass flux; composition in the mixture transport properties; and finally, temperature in the difference between wire and fluid,  $T_s - T_\infty$ . Therefore, Equation 2.7 serves as a theoretical baseline in this study.

An empirical correlation for concentration probe calibration data has eluded researchers, as noted by Brown and Rebollo (3:650). However, promising work by Tanis indicates that it is possible to correlate calibration constants for  $Nu_d$  under conditions where sensor  $Re_d$  is changing for a fixed molar fraction of helium in a mixture (10). Initial results have yielded the equation

$$Nu_d \left( \frac{T_s - T_\infty}{T_\infty} \right)^{0.17} = \left[ A \left( Re_d^{0.45} \right)^2 + B Re_d^{0.45} + C \right] Pr^{0.3} (x_{He} + 1)^{[0.13 Re_d - 0.55]} \quad (2.9)$$

where  $A$ ,  $B$  and  $C$  are calibration constants, and  $x_{He}$  is the molar fraction of helium in an air/helium mixture. In this study, it is necessary to determine the calibration constants for Equation 2.9 based on data obtained with the tank discharge calibration method.  $Nu_d$  takes the general form

$$Nu_d = Nu_d(T_s/T_\infty, Re, Pr, x_{He}) \quad (2.10)$$

Inspection of Equations 2.5, 2.8 and 2.10 shows the gradual restructuring of variables needed to define the experimental correlations. It is no wonder that concentration probe calibration correlations have defied characterization for so long.

Next, the determination of transport properties needs to be addressed. The mixture transport properties  $k_f$  and  $\mu_f$  must be determined using a semiempirical formula (4:24,258) of the form

$$k_f = k_{mix} = \sum_{i=1}^n \frac{x_i k_i}{\sum_{j=1}^n x_i \Phi_{ij}} \quad (2.11)$$

and similarly for viscosity

$$\mu_f = \mu_{mix} = \sum_{i=1}^n \frac{x_i \mu_i}{\sum_{j=1}^n x_i \Phi_{ij}} \quad (2.12)$$

in which

$$\Phi_{ij} = \frac{1}{\sqrt{8}} \left( 1 + \frac{M_i}{M_j} \right)^{-0.5} \left[ 1 + \left( \frac{\mu_i}{\mu_j} \right)^{0.5} \left( \frac{M_j}{M_i} \right)^{0.25} \right]^2 \quad (2.13)$$

In these expressions,  $x_i$  and  $x_j$  are species molar fractions,  $\mu_i$  and  $\mu_j$  are the viscosities for the separate species and  $M_i$  and  $M_j$  are species molecular weights. These formulas work very well for low density gas mixtures. Appendix A contains plots of the mixture properties used in this study as a function of helium molar fraction.

With transport property dependence on concentration firmly established, a solid relationship is developed between Equation 2.4 and Equation 2.9. This relationship forms the basis for the practical use of tank discharge calibration data, although the utility of Equation 2.4 extends to the steady flow calibration method as well.



### *III. Experimental Apparatus*

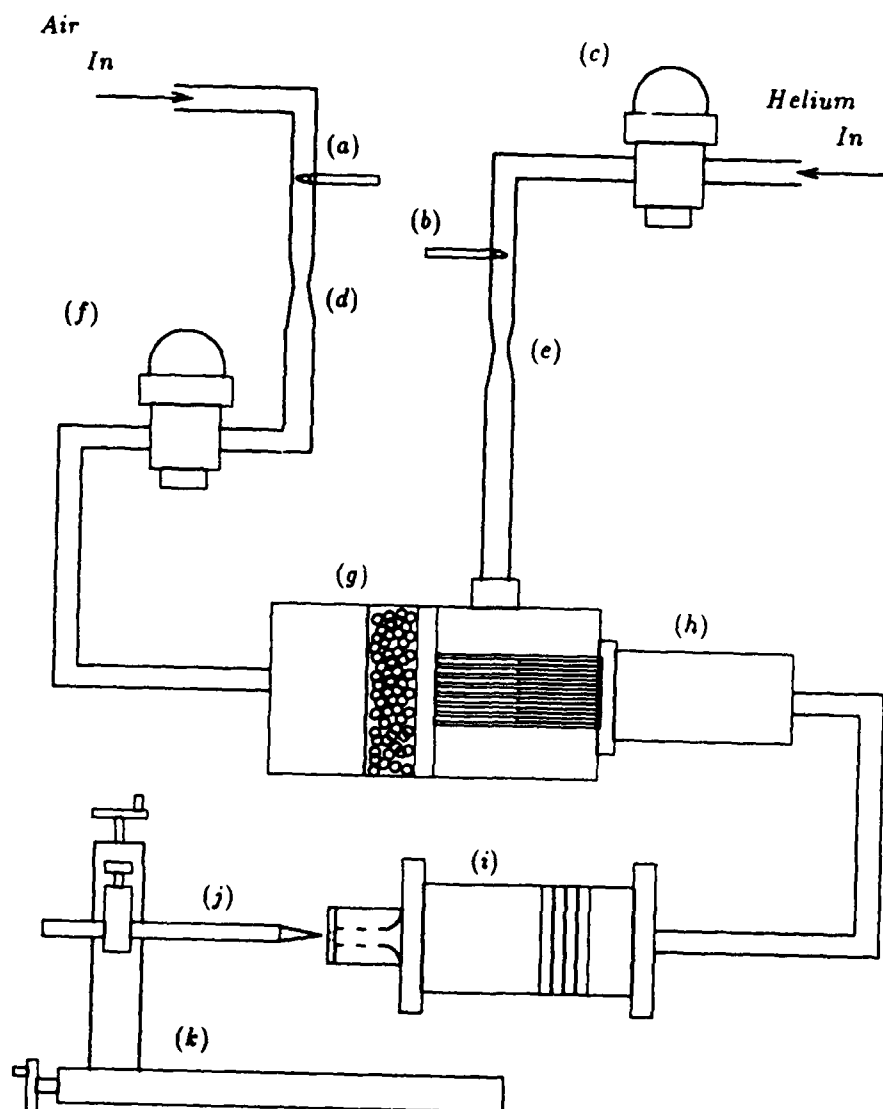
This study required a thoroughly mixed, binary source flow of helium and air. An apparatus to supply such a flow was developed and built. The principle of operation is simple — the mass flow rates of two streams of non-reacting gases are measured separately, then they are mixed thoroughly, resulting in a mixture of known mass and molar concentration for each of the species. The mixture supply system was one of six major systems that comprised the entire test apparatus. The other five systems were the steady flow test system, the tank discharge test system, the hot wire anemometer system, the concentration probe system and the data acquisition system.

#### *3.1 Mixture Supply System*

The mixture supply system consisted of two major subsystems, the constituent metering subsystem and the constituent mixing subsystem. Helium and air mass flow rates were measured and controlled separately by the metering subsystem before being combined by the mixing subsystem.

*3.1.1 Constituent Metering Subsystem* Constituent gas flow was measured and controlled by the metering subsystem. Stainless steel tubing was put in place to provide a supply of clean, dry compressed air from the laboratory high pressure supply facility. Air supply pressure was maintained nominally at 100 psig by two compressors. Helium was supplied to the system through high pressure stainless steel tubing from a compressed helium cylinder.

The helium and air flows were controlled through the use of two high pressure dome valves working in combination with two finely adjustable Grove regulators, one combination of regulator and dome valve for each flow. Figure 3.1 depicts the mixture supply system as it feeds into the steady flow test system. Both gas flows passed through machined convergent, classical venturi tubes in order to measure mass flow rate. The venturi tubes were placed well downstream from valves, elbows and other flow disturbing elements, fully complying with ASME guidelines for the placement of venturi tubes in flow



(a)&(b), thermocouples; (c)& (f), dome valves; (d)&(e), venturi tubes; (g), mixing device; (h), mixing chamber; (i), stilling chamber and nozzle; (j), probe; (k), probe holder

Figure 3.1. Schematic of mixture supply and steady flow test systems

systems. Determination of mass flow rate through the venturi tubes required the following information: the upstream static pressure and temperature, the difference between static pressure upstream of the venturi and at the venturi throat, the venturi tube physical dimensions and its discharge coefficient. Upstream static temperature was measured by a copper/constantan thermocouple referenced to an electronic ice point. The upstream static pressure was measured at the entrance to the convergent section of each venturi and differential pressure transducers were connected from these points to each venturi throat tap.

*3.1.2 Constituent Mixing Subsystem* The constituent mixing subsystem was an adaptation of a device originally used by Zakanycz in his study of the turbulent mixing of binary gases (11:15). Figure 3.2 depicts the device as used by Zakanycz. Minor modifications were made at the supply and exit interfaces in order to integrate the mixing device with the system. Referring again to Figure 3.2, air entered at the left end of the cylindrically shaped mixer and encountered a section of beads (for flow spreading) before entering the bank of small tubes. Helium entered the device at a boss protruding from the side of the cylinder and flowed into a chamber that in turn supplied small tubes interspersed at regular intervals between the air tubes. All the tubes exited at the right end of the device into the mixing chamber, where the streams of helium intermingled with the streams of air.

### *3.2 Steady Flow Test System*

Gaseous mixture produced in the mixing device was piped to the steady flow test system, consisting of an instrumented stilling chamber, a nozzle and a probe holder. The chamber was instrumented with a iron/constantan thermocouple connected to a digital readout box and a pressure transducer referenced to atmosphere. Flow entering the chamber passed through a series of screens for flow straightening before encountering a smoothly transitioned inlet to the ASME flow nozzle. Two options for nozzle exit diameter were available, 0.6 in and 0.125 in. The clear plastic chamber was adapted from a factory-made hot wire calibrating device for use with this apparatus. The probe holder was capable of

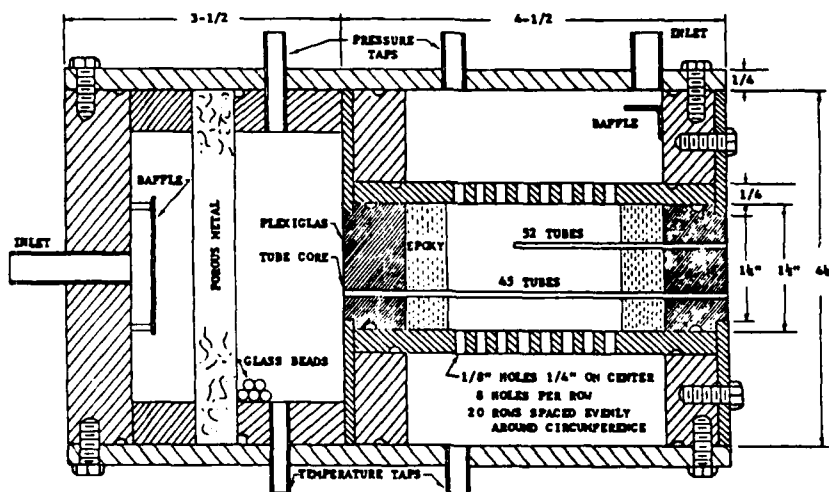


Figure 3.2. Constituent mixing device for helium and air streams

positioning in three axes using screw-actuated mechanisms. A screw-tightened jaw was used to secure the probe to the probe holder.

### 3.3 Tank Discharge Test System

A cylindrical aluminum tank with a 6.5 in diameter and 7.5 in length was the central component of the discharge test system, as illustrated in Figure 3.3. At one end of the tank, valves were attached so that tank evacuation, helium charging and air charging were easily accomplished, as shown in Figure 3.3. At the other end of the tank, a ball valve controlled the mixture outflow into a flexible plastic tube leading to the probe entrance. This tube was connected to a compression fitting capable of slipping over the probe tip and sealing against the probe support tube with an O-ring. The tank was instrumented with an iron/constantan thermocouple connected to digital readout box and a pressure transducer referenced to atmosphere.

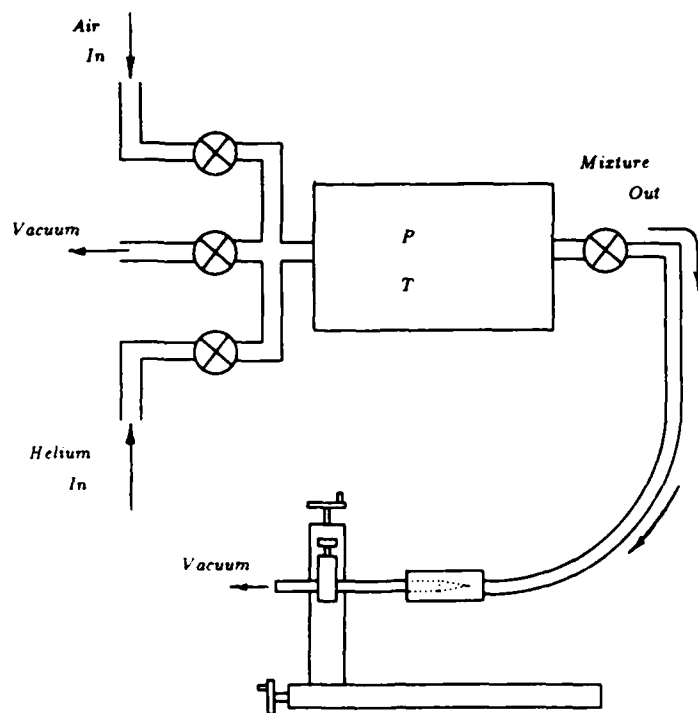


Figure 3.3. Tank discharge schematic

#### 3.4 Hot Wire Anemometer System

The probe sensor was attached to a Thermal Sciences, Inc. (TSI) Model 1051 hot wire anemometer as one resistive arm of a bridge circuit. A negative-feedback amplifier kept the bridge in balance by changing the supply voltage to keep the sensor arm at a constant temperature.

#### 3.5 Concentration Probe

The concentration probe consists of a plastic forebody covered by a machined brass inlet cone at the forward end. The rearward end is inserted into an 8-inch long stainless steel tube. The forebody supplies structural support to the needle size sensor "stings" as well as the sensor chamber thermocouple and total pressure tap. Figure 3.4 depicts the major features of the probe. The probe used in this study was designed and built by Tanis (10), and modified by the investigator to include the chamber thermocouple. The sensor is a 0.0005 in diameter tungsten wire, electrically welded to the stings. It was designed for use in supersonic streams, hence the probe inlet and the diverging channel

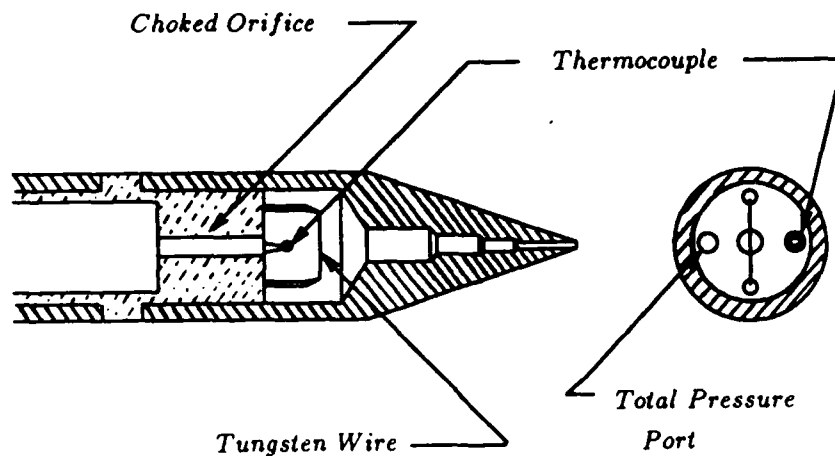


Figure 3.4. Basic concentration probe

behind the inlet are designed to avoid the occurrence of a bow shock at the tip. Swallowing the shock ensures that a stream tube equal in area to the probe inlet capture area enters the probe undisturbed (9:2). In this way, there is little chance for spillage *around* the inlet—a condition that could lead to erroneous readings since the light gas would be deflected by the spillage more than the heavy gas.

### 3.6 Data Acquisition System

The data acquisition system was comprised of a Zenith 248 personal computer connected to a Datalab 1200 (DL1200) data collection system by an IEEE-488 interface bus. Software was designed to control the DL1200 through the IEEE-488 bus and to process the binary data it produced. The DL1200 has eight channels and can collect 4096 data points on each channel simultaneously, for sample rates ranging from 500 kHz to 50 Hz. Six of the input channels originated from six Endevco signal conditioner outputs which consisted of signals from two venturi static pressure transducers, two venturi differential pressure transducers, one stilling chamber pressure transducer and the probe

chamber total pressure transducer. The remaining two channels were connected to the outputs of the venturi thermocouple amplifiers.

## IV. Experimental Procedures

The procedures executed for this study are classified as either general or specific. Procedures that were done repetitively or spanned more than one specific area are grouped in the general category. Common laboratory procedures such as pressure transducer calibration or atmospheric pressure measurement have been excluded for the sake of brevity. Specific procedures covered in this chapter include two probe calibration procedures: the steady flow procedure and the tank discharge procedure. Data were collected using both procedures *with the same probe*, so that the two methods could be compared.

### 4.1 General Procedures

**4.1.1 Venturi Calibration** Each of the two venturi tubes were calibrated with respect to their unique discharge coefficients.  $C_d$  was determined by allowing only one gas to pass through the system at a time and metering the mass flow rate at the exit of the system by means of a choked converging nozzle. The details on determination of  $C_d$  are in Appendix B.

**4.1.2 Hot Wire Anemometer Preparation** The hot wire operating resistance was found by first heating the wire (externally, using a heat gun), and then observing its resistance as a function of temperature as it cooled. That relationship was then used to determine the resistance,  $R_s$ , corresponding to the desired sensor operating temperature (940 R.) Further detail on the remainder of the rather extensive preparation procedure is described in the operating manual prepared by TSI (8).

**4.1.3 Start-up** Electronic equipment was powered up to allow sufficient time for warm-up and stabilization. All joints were tightened and leak-checked to protect against the loss of mass between the venturi tube and the flow nozzle at the system exit. One data collection run was made with all instruments exposed to ambient conditions (a *zero* run). This provided an atmospheric reference point for absolute pressure measurements.



#### *4.2 Steady Flow Probe Calibration Procedure*

The concentration probe centerline was positioned on the exit centerline of the steady flow test system, facing directly upstream. During the entire set of data runs, sensor chamber total pressure was maintained at a constant value (selected values ranged from 4 to 6 psia), while helium mole fraction was varied from 0 to 1. In order to maintain a choked orifice in the probe, an absolute pressure of not more than 30 mm Hg was maintained behind the orifice. This was accomplished by attaching a vacuum pump to the end of the probe body. A detailed description of the steady flow data collection procedure follows.

The start-up procedure described in the General Procedures section was first executed. Then, the first data collection run was made with pure air, steadily increasing the flow rate until the desired sensor chamber total pressure was attained. When the flow was properly adjusted, an external trigger signal was sent to the DL1200 and a set of points was recorded. Four thousand ninety-six data points were taken by the DL1200 at a sample rate of 1kHz for each run. When the data recording was complete, the DL1200 was commanded to download the raw data by the computer program. While the acquisition system downloaded data for hard disk storage, the flow was readjusted. This was accomplished by backing off the air mass flow rate and adding helium flow until the sensor chamber total pressure once again reached its desired level. Increasingly larger flows of helium along with smaller flows of air were mixed until the flow was pure helium. The pure helium run required evacuation of the flow system up to the air dome valve, in order to ensure that no residual air was contained in the volume from the dome valve to the mixer. It was found that if this procedure was not followed, residual air contaminated the pure helium run.

#### *4.3 Tank Discharge Probe Calibration Procedure*

The tank was normally charged to a mixture total pressure of about 50 psia. In the case of all the tank volume charging operations, tank pressure and temperature values were taken only after they were allowed to stabilize with environment. First, a zero voltage run was conducted (as described previously), then the tank and all lines were evacuated. After sufficient evacuation of the tank, pure air was admitted. Once the tank was charged with air and stabilized, tank pressure and temperature readings were taken and helium

was admitted. Upon stabilization, the pressure and temperature of the mixture were recorded. Those two sets of data provided the information necessary for calculation of molar concentration. Next, the mixture outlet valve was opened, thus exposing the probe to gas from the tank. The DL1200 was triggered to record after allowing 2 seconds for the gas to travel up the plastic tube to the probe. The DL1200 was set to take 4096 samples over an 81 second period. During the downloading of data files to the computer, the mixture control valve was closed and the tank and lines (including the probe) were again evacuated. For subsequent runs, different proportions of helium and air were added to the tank in order to achieve a range of concentration values.

## V. Results

Data were collected to determine a relationship between the concentration of helium in an air/helium mixture and hot wire sensor heat loss. For both the steady flow calibration method and the tank discharge calibration method, sensor heat loss is directly related to the supply voltage applied to a bridge circuit, and is given by the expression

$$Q = I^2 R_s = \frac{V_{br}^2 R_s}{(R_s + R_{ser})^2} \quad (5.1)$$

Equation 5.1 is an extension of Equation 2.1 that provides  $Q$  in terms of the measurable quantity,  $V_{br}$ , the bridge supply voltage, and two resistances fixed at the beginning of operation,  $R_s$  and  $R_{ser}$ .  $R_s$  was identified earlier as the sensor operating resistance while  $R_{ser}$  is a fixed resistance in series with  $R_s$  in the bridge circuit. Therefore, the steady flow method and the tank discharge method rely upon this relationship to quantify wire heat loss in terms of a measurable voltage. Since the same sensor was used for both methods, the basis of comparison between the two methods rests on the helium molar fraction,  $x_{He}$ , versus wire heat loss,  $Q$ , relationship. Hence, the results are given in terms of this relationship.

Although determination of  $Q$  through the ohmic relationship is the same for both methods, determination of the relationship between  $Q$  and  $x_{He}$  is quite different. For this reason, the results for the steady flow method and the tank discharge method are first presented separately, and then brought together for comparison purposes.

### 5.1 Steady Flow Calibration Method Results

All pressure and temperature voltage signals for the venturi flowmeters, along with the hot wire bridge voltage were stored on the computer hard disk in binary format for post-processing. They were then converted, using software, from digital integer values back into voltage values. 4096 voltage readings per channel were then averaged to obtain reduced voltages. Mass flow rate through the venturi tubes was determined using the

differential pressure fluid meter equation (2:63)

$$\dot{m} = \frac{C_d}{(1 - \beta^4)^{0.5}} Y_r a (2g_c \rho_1 \Delta p)^{0.5} \quad (5.2)$$

After  $\dot{m}$  for each separate flow was determined, the helium and air flows were summed to obtain the mixture mass flow rate,  $\dot{m}_{mix}$ . The molar fraction of helium in the mixture could then be obtained by use of the equation

$$x_{He} = \frac{\dot{m}_{He}}{\dot{m}_{mix}} \left( \frac{M_{mix}}{M_{He}} \right) \quad (5.3)$$

$M_{mix}$  and  $M_{He}$  are the molecular weights of the air/helium mixture and helium respectively. In this way, a direct relationship between  $x_{He}$  and  $V_{br}$  (and thus,  $Q$ , through Equation 5.1) was made for a given data point.

Figure 5.1 is the typical calibration curve that resulted from the reduced data. Figure 5.2 shows two of these curves, each with a different value of total pressure in the sensor chamber. This is not a disturbing observation nor one that cannot be explained. Changing  $P_0$  or  $T_0$  causes changes in mass flow rate through the choked orifice, and thus mass velocity past the wire (which is directly related to a change in  $Re_d$ .) This effect has not been *eliminated* by the design of the probe, but it has been *quantified* and thus can be isolated by the calibration curve from concentration effects. These results have shown that the steady flow system produces viable calibration curves.

## 5.2 Tank Discharge Method Results

Processing of the raw data was identical to the steps followed in the steady flow data reduction process, up to the point where mass flow rates were calculated. In the tank discharge method, however, concentration of helium was determined by use of the perfect gas law applied to the fixed tank volume such that

$$x_{He} = \frac{n_{He}}{n_{mix}} = \frac{P_{He}}{P_{mix}} \frac{T_{mix}}{T_{He}} \quad (5.4)$$

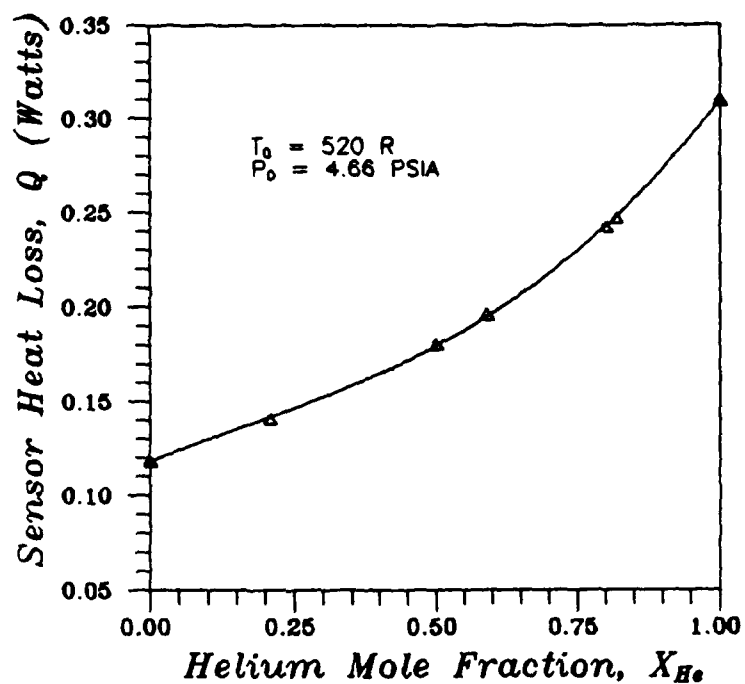


Figure 5.1. Steady flow calibration curve

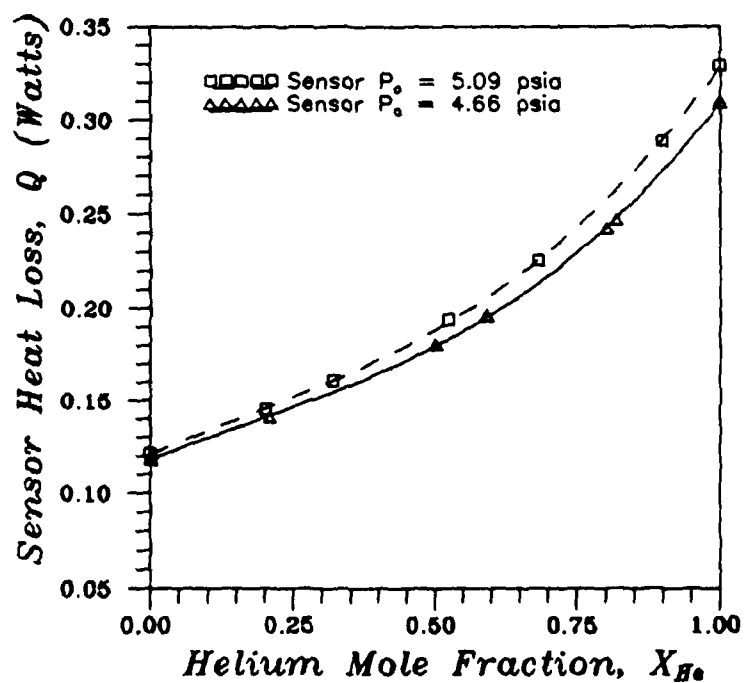


Figure 5.2. Steady flow curves with different sensor  $P_0$  values

As the tank released its charge of gas mixture, sets of data were collected where concentration was constant and sensor total pressure (and temperature) continuously dropped, in contrast with the steady flow method where sensor total pressure remained constant. Several of these sets were collected for different concentrations. Figure 5.3 shows four sets of data points plotted with  $Nu$  as a function  $Re$ . A correlation of this set of constant

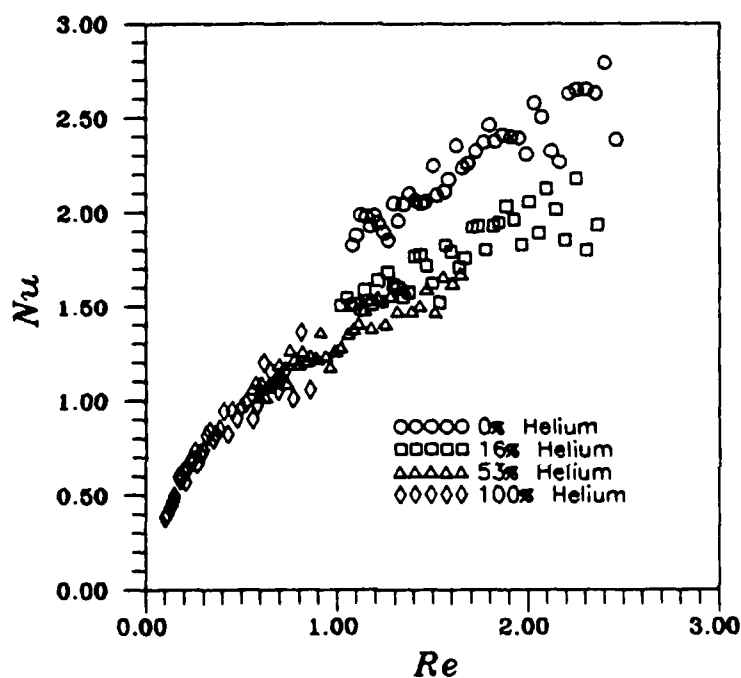


Figure 5.3. Reynolds versus Nusselt numbers from tank discharge data

concentration curves was necessary if the tank discharge method was to be compared with the steady flow method. Thus, Equation 2.9 was applied and rearranged slightly in order to define  $Y$  such that

$$Y = \frac{Nu_d \left( \frac{T_d - T_\infty}{T_\infty} \right)^{0.16}}{Pr^{0.38} (x_{He} + 1)^{[0.13Re_d - 0.55]}} = \left[ A (Re_d^{0.45})^2 + B Re_d^{0.45} + C \right] \quad (5.5)$$

or in general,

$$Y = f(Re^{0.45}) \quad (5.6)$$

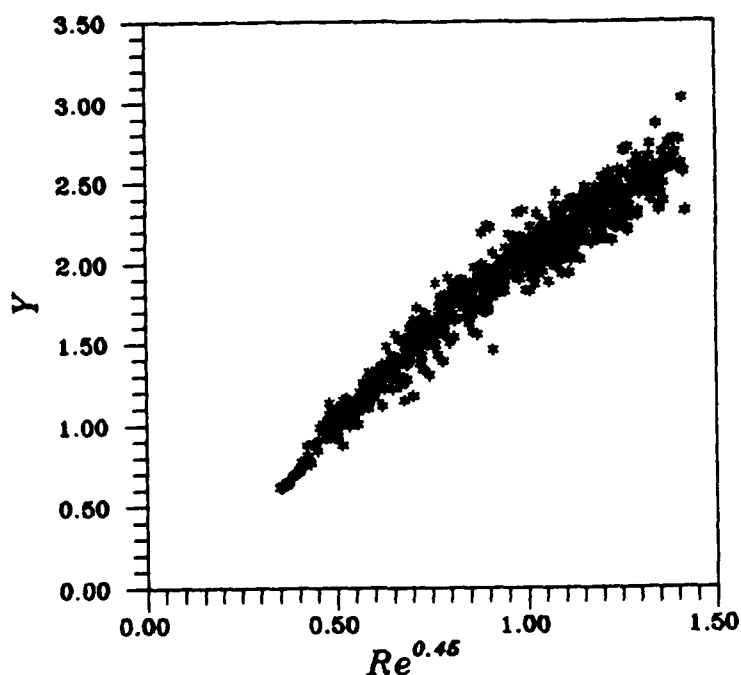


Figure 5.4. Tank discharge method: sensor heat loss correlation

For a better fit, the exponents of  $Pr$  and the  $(T_s - T_\infty)/T_\infty$  ratio were adjusted slightly from those given in Equation 2.9. Figure 5.4 shows how the separate concentration curves of Figure 5.3 are collapsed together by the correlation. The point scatter that is evident in both figures is the result of bridge voltage fluctuation. Steady flow data reduction effectively captured and averaged that fluctuation. The tank discharge data was not averaged and hence assigned a data point to each discrete voltage sample. This is illustrated in Figure 5.5, where it is shown that the procedure used with the tank discharge method was destined to collect scattered bridge voltage points over a sampling interval, since mean bridge voltage was dropping with time. A discrete voltage had to be assigned to the flow condition *at that instant*. Since bridge voltage was directly related to heat loss, and heat loss was directly related to  $Nu_d$ , the effect of this voltage fluctuation was to scatter the points in Figure 5.4. In contrast, flow conditions were not changing with the steady flow method, therefore fluctuating bridge voltages could be *averaged* over a short *sampling interval*. The flow dynamics associated with the entrance and cavity of this *particular* probe are suspected to have caused the sensor's fluctuating response, although the *specifics* remain to be determined. A second degree polynomial curve fit through the data points in

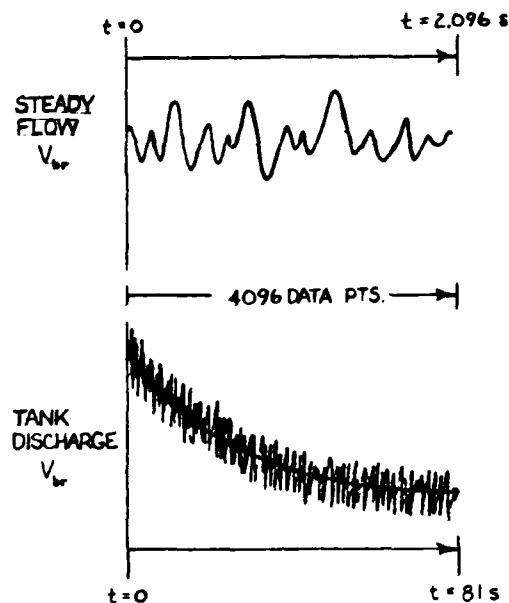


Figure 5.5. Comparison of one sample interval, steady flow vs. discharge method

Figure 5.4 yielded the function

$$Y = -.75657 + 3.19978 Re^{.45} - .399196 (Re^{.45})^2 \quad (5.7)$$

with the expression for  $Y$  given by Equation 5.5. This relationship was used to generate the tank discharge calibration curve for comparison with the steady flow calibration curve. It should be noted that the constants in Equation 5.7 are constants for the particular sensor used in this investigation.

### 5.3 Comparison of Steady Flow and Tank Discharge Results

The steady flow operating conditions of Figure 5.1 ( $T_0$ ,  $P_0$ ) were applied to the correlation given by Equation 5.5, thereby holding Reynolds number and temperature constant so that  $Nu_d = Nu_d(x_{He})$ . The following equation for  $Q_{td}$  based on the tank



discharge correlation resulted:

$$Q_{td} = \frac{k_f A_{cyl} (T_s - T_\infty) Y Pr^{0.38} (x_{He} + 1)^{[0.13 Re_d - 0.55]}}{d \left( \frac{T_s - T_\infty}{T_\infty} \right)^{0.16}} \quad (5.8)$$

A relationship between  $Q$  and  $x_{He}$  for constant  $P_0$  and  $T_0$  based on tank discharge data was now established, so the two could be compared directly.

The upper curve of Figure 5.6 is the curve generated by varying concentration in Equation 5.8. The lower curve came directly from Figure 5.1. For a given value of wire heat loss, there is an almost uniform 0.05 difference in helium molar fraction between the steady flow method and the tank discharge method, with the tank discharge method posting consistently lower values. Steady flow values for heat loss from the sensor are in very close agreement with the tank discharge curve, especially considering two factors: the very different ways that concentration was determined in each method, i.e. ratio of flow rates versus perfect gas law in a fixed volume; and the uncertainty produced by the point scatter in the tank discharge method. This demonstration indicates a need to further study the internal flow characteristics of the probe and perhaps devise a means to eliminate the velocity fluctuations the sensor is experiencing. The close agreement seen in Figure 5.6 is evidenced again in Figure 5.7, in this case at a different operating condition (different  $Re_d$ ). The third curve plotted on Figure 5.7 was generated from King's law by a manipulation of Equation 2.7, which yielded

$$Q_k = \frac{k_f}{d} A_{cyl} (T_s - T_\infty) \left[ \frac{1}{\pi} + \left( \frac{2}{\pi} Re_d Pr \right)^{0.5} \right] \quad (5.9)$$

Although King's law was based on potential flow theory, its shape is very similar to the curves obtained from experimental data. The fact that the heat loss predicted by King's law is *less* than the experimentally measured value, may be indicative of the theoretical assumption that all the heat transfer is convective. The actual case includes additional heat loss from the sensor through conduction down the mounting stings and heat loss through radiation. The fact that the shape is similar indicates that the influence of concentration

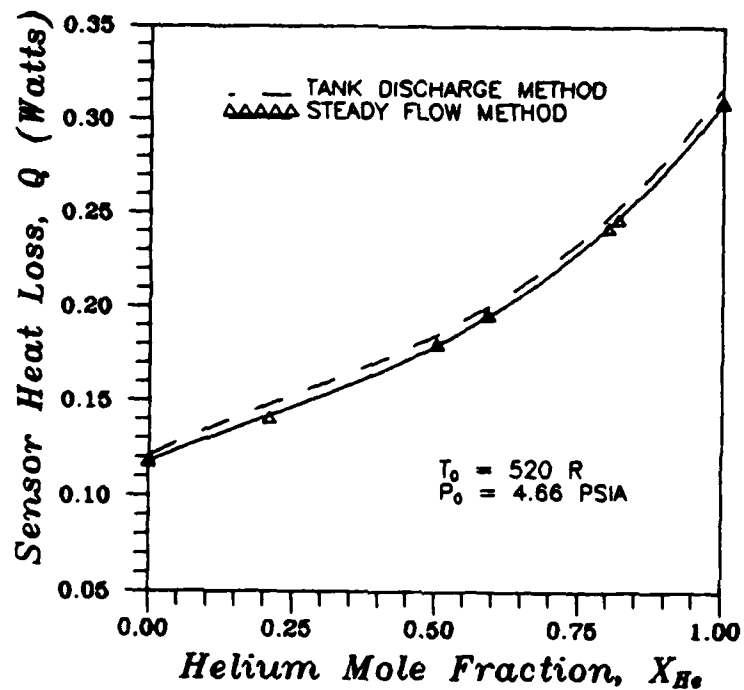


Figure 5.6. Calibration method comparison: steady flow vs. tank discharge

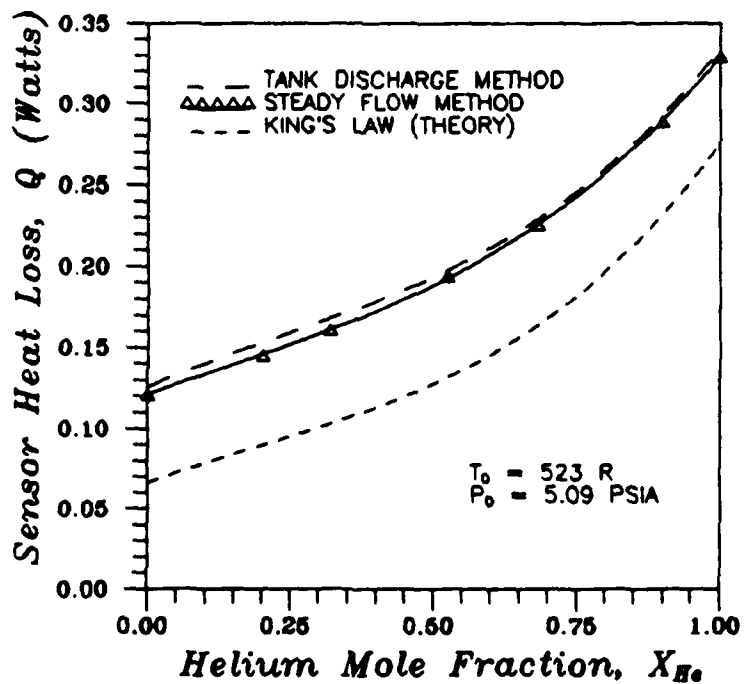


Figure 5.7. Calibration method comparison and King's law

on heat loss is directly related to the influence of concentration of the transport properties inherent in  $Re$  and  $Pr$ .

## *VI. Conclusions and Recommendations*

### *6.1 Conclusions*

The task of establishing a steady flow alternative to the tank discharge calibration method was completed. Analysis of the data gathered using both methods led to the following conclusions:

1. The steady flow calibration curve and the tank discharge calibration curve showed close agreement for constant sensor chamber total pressure. Therefore, either method can be used for calibration of a concentration probe.
2. Although King's law is based on potential flow theory, the shape of its curve was very similar to the calibration curves obtained from experimental data. The higher experimental heat loss values are probably manifestations of the fact that King's law does not take into account conduction and radiation heat losses.

### *6.2 Recommendations*

Work in this area has by no means been exhausted. Therefore, the following topics are suggested for continued study:

1. Study the internal flow characteristics of the probe to better understand the mechanisms involved.
2. Conduct a parametric study on probe sensor cavity design to optimize probe sensitivity and reduce susceptibility to velocity fluctuations.
3. Extend the capability of the steady flow system to include supersonic flow calibration.
4. Apply Tanis' correlation to steady flow calibration.

## Appendix A. *Properties of Mixtures*

The following plots demonstrate how the transport properties  $\mu_f$  and  $k_f$  vary with concentration for a constant fluid temperature of 520 R, in accordance with Equation 2.13, Equation 2.14 and Equation 2.15. Although not a transport property, specific heat is included because when joined together with the two transport properties, it forms Prandtl number, the ordinate of the final plot, Figure A.4.

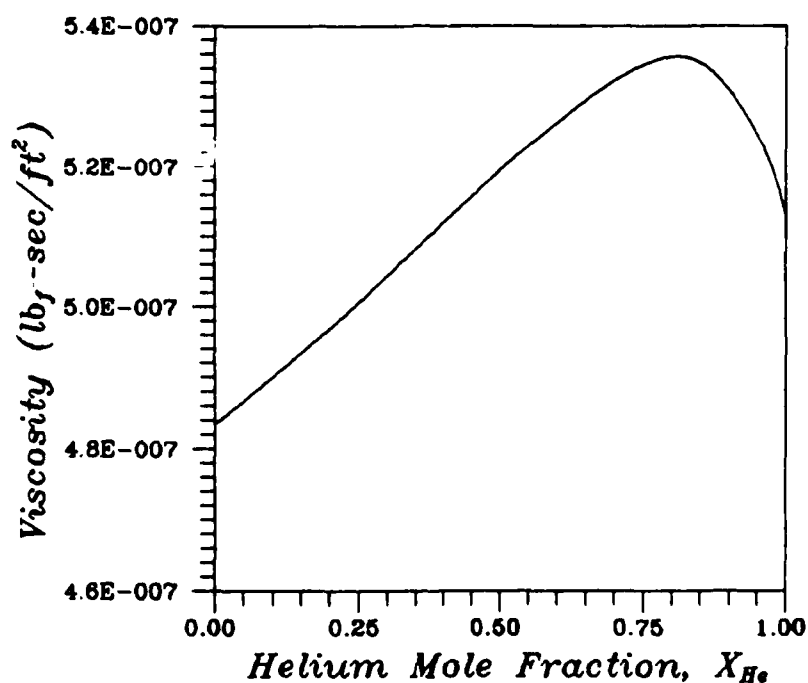


Figure A.1. Mixture viscosity as a function of helium molar fraction

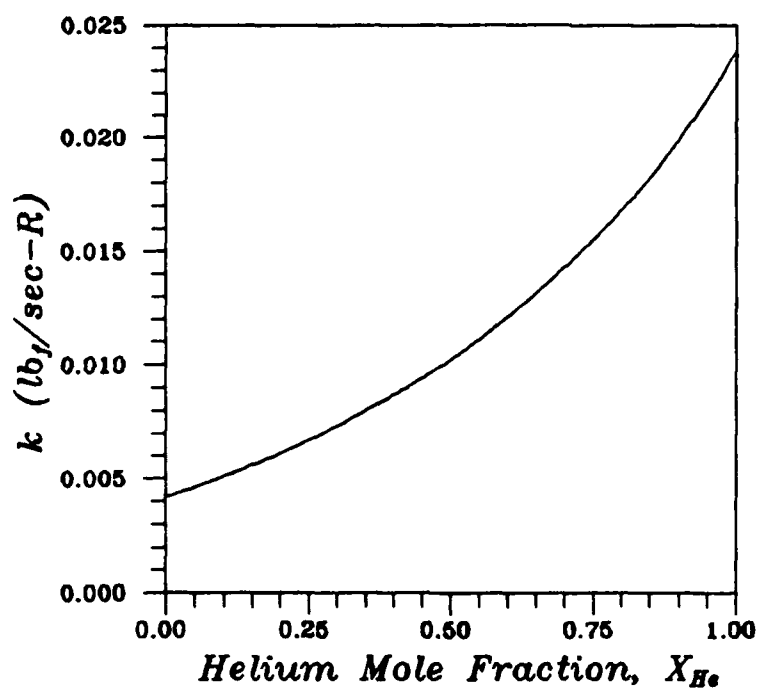


Figure A.2. Mixture thermal conductivity as a function of helium molar fraction

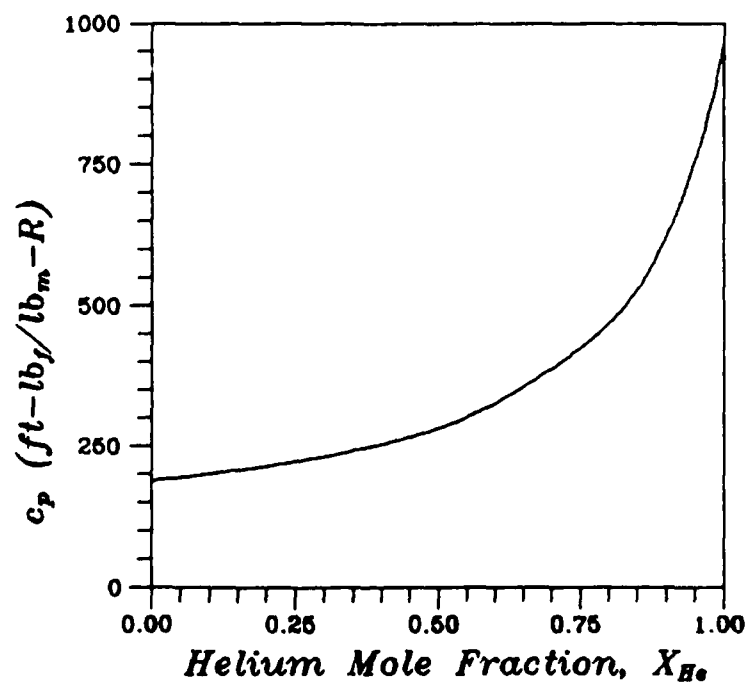


Figure A.3. Mixture specific heat as a function of helium molar fraction

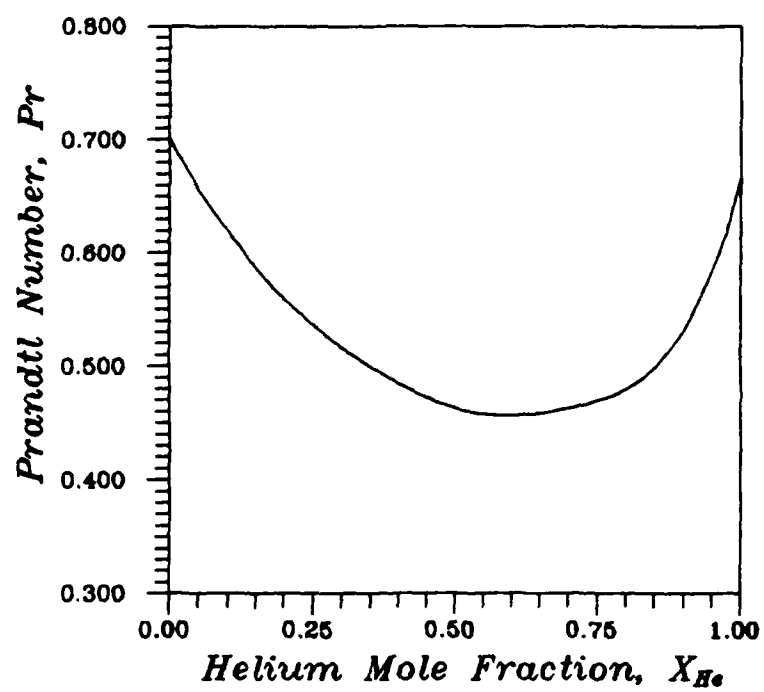


Figure A.4. Mixture Prandtl number as a function of helium molar fraction

## Appendix B. Venturi Calibration

The venturi tube flowmeters were calibrated through the measurement of mass flow rate exiting a choked, converging nozzle at the end of the steady flow mixing system. Two critical assumptions were made: the coefficient of discharge of the sonic nozzle,  $C_{dsn}$ , was known to be 0.968 (6:34); and any mass leakage between the venturi tube and the sonic nozzle was assumed to be negligible. This assumption required meticulous care in making sure that all joints were tight and sealed. With that accomplished, conservation of mass could be applied to the system such that

$$\dot{m}_{sonicnoz} = \dot{m}_{venturi} \quad (B.1)$$

It is known that

$$\dot{m}_{sonicnoz} = C_{dsn} A_{snt} \frac{P_0 \Gamma}{\sqrt{RT_0 g_c}} \quad (B.2)$$

where

$$\Gamma = \sqrt{\gamma \left( \frac{2}{\gamma + 1} \right)^{\frac{\gamma+1}{\gamma-1}}} \quad (B.3)$$

From Equation 5.2 it is also known that

$$\dot{m}_{venturi} = \frac{C_{dv}}{(1 - \beta^4)^{0.5}} Y_r a (2g_c \rho_1 \Delta p)^{0.5} \quad (B.4)$$

Another way of expressing mass flow rate is

$$\dot{m}_{sonicnoz} = C_{dsn} \dot{m}_{sntheor} \quad (B.5)$$

by the definition of discharge coefficient. Similarly,

$$\dot{m}_{venturi} = C_{dv} \dot{m}_{utheor} \quad (B.6)$$

for the venturi mass flow rate. Substituting these expressions into the very first equation yields

$$\frac{\dot{m}_{sntheor}}{\dot{m}_{utheor}} = \frac{C_{dv}}{C_{dsn}} \quad (B.7)$$



which can be expressed as

$$C_{dv} = C_{dsn} \frac{\dot{m}_{sntheor}}{\dot{m}_{vtheor}} \quad (B.8)$$

The theoretical mass flow rates were determined from measurable quantities, functions of pressure, temperature, throat area and  $\gamma$ . Therefore, with  $C_{dsn} = 0.968$  (mentioned above),  $\dot{m}_{sntheor}$  measured from stagnation values upstream of the sonic nozzle and  $\dot{m}_{vtheor}$  determined from measurements at the venturi tube, it was possible to determine  $C_{dv}$ .

### *Bibliography*

1. Adler, D. "A Hot-Wire Technique for Continuous Measurement in Unsteady Concentration Fields of Binary Gaseous Mixtures," Journal of Physics E, 5: 163-169 (1972).
2. ASME Fluid Meters: Their Theory and Applications. Edited by Howard S. Bean. New York: ASME, 1971.
3. Brown, G. L. and Rebello, M. R. "A Small Fast Response Probe to Measure Composition of a Binary Gas Mixture," AIAA Journal, 10: 649-652 (May 1972)
4. Bird, R., Stewart, W. E. and Lightfoot, E. N. Transport Phenomena. New York: John Wiley and Sons, Inc., 1960.
5. Collis, D. C. and Williams, M. J. "Two-Dimensional Convection from Heated Wires at Low Reynolds Number," Journal of Fluid Mechanics, 6: 357-384 (October 1959)
6. Idelchik, I. E. Handbook of Hydraulic Resistance. New York: Hemisphere Publishing Corporation, 1986.
7. Lomas, C. G. Fundamentals of Hot Wire Anemometry. New York: Cambridge University Press, 1986.
8. Model 1050 Constant Temperature Anemometer Instruction Manual. St. Paul: Thermal Sciences Inc., 1967.
9. Ng, W. F., Kwok, F. T., Ninnemann, T. A. "A Concentration Probe for the Study of Mixing in Supersonic Shear Flows," AIAA/ASME/SAE/ASEE 25th Joint Propulsion Conference: AIAA-89-2459 (July 1989)
10. Tanis, F., PhD Candidate. Personal interviews, School of Engineering, Air Force Institute of Technology, Wright-Patterson AFB OH, 4 January through 15 November 1989.
11. Zakanycz, S. Turbulence and the Mixing of Binary Gases. PhD dissertation. Ohio State University, OH, 1971.

## Vita

Captain George R. Stoller Jr. [REDACTED]

[REDACTED] After graduating in 1979 from Westminster Academy, a Christian high school located in Fort Lauderdale, Florida, George pursued a pre-engineering degree at Broward Community College. Prior to continuing his *formal* education at the University of Florida, he spent slightly over one year working in marine hydraulics. The University of Florida conferred on Capt Stoller the degree of Bachelor of Science in Mechanical Engineering in August 1985, and he was immediately commissioned as a Second Lieutenant in the United States Air Force. After serving as a staff officer for the DCS/Plans of Air Force Space Command for two and one half years, Capt Stoller reported to the Air Force Institute of Technology for training in May 1988.

[REDACTED]

[REDACTED]

REPORT DOCUMENTATION PAGE

Form Approved  
OMB No. 0704-0188

1a. REPORT SECURITY CLASSIFICATION UNCLASSIFIED			1b. RESTRICTIVE MARKINGS		
2a. SECURITY CLASSIFICATION AUTHORITY			3. DISTRIBUTION/AVAILABILITY OF REPORT Approved for public release; distribution unlimited		
2b. DECLASSIFICATION/DOWNGRADING SCHEDULE			5. MONITORING ORGANIZATION REPORT NUMBER(S)		
4. PERFORMING ORGANIZATION REPORT NUMBER(S) AFIT/ENY/GAE/89D-37			7a. NAME OF MONITORING ORGANIZATION		
5a. NAME OF PERFORMING ORGANIZATION School of Engineering		6b. OFFICE SYMBOL (if applicable) AFIT/ENY		7b. ADDRESS (City, State, and ZIP Code)	
6c. ADDRESS (City, State, and ZIP Code) Air Force Institute of Technology Wright-Patterson AFB OH 45433-6583			9. PROCUREMENT INSTRUMENT IDENTIFICATION NUMBER		
8a. NAME OF FUNDING/SPONSORING ORGANIZATION		8b. OFFICE SYMBOL (if applicable)		10. SOURCE OF FUNDING NUMBERS	
8c. ADDRESS (City, State, and ZIP Code)		PROGRAM ELEMENT NO.		PROJECT NO.	TASK NO.
					WORK UNIT ACCESSION NO.
11. TITLE (Include Security Classification) DEVELOPMENT OF AN ALTERNATIVE CONCENTRATION PROBE CALIBRATION METHOD					
12. PERSONAL AUTHOR(S) George R. Stoller, Jr., B.S., Capt, USAF					
13a. TYPE OF REPORT MS Thesis		13b. TIME COVERED FROM _____ TO _____		14. DATE OF REPORT (Year, Month, Day) 1989 December	
				15. PAGE COUNT 43	
16. SUPPLEMENTARY NOTATION					
17. COSATI CODES			18. SUBJECT TERMS (Continue on reverse if necessary and identify by block number)		
FIELD	GROUP	SUB-GROUP	Supersonic Flow Concentration		
20	04		Gas Flow		
07	04				
19. ABSTRACT (Continue on reverse if necessary and identify by block number)					
Thesis Advisor: William C. Elrod Professor Department of Aeronautics and Astronautics					
20. DISTRIBUTION/AVAILABILITY OF ABSTRACT <input checked="" type="checkbox"/> UNCLASSIFIED/UNLIMITED <input type="checkbox"/> SAME AS RPT. <input type="checkbox"/> DTIC USERS			21. ABSTRACT SECURITY CLASSIFICATION UNCLASSIFIED		
22a. NAME OF RESPONSIBLE INDIVIDUAL William C. Elrod, Professor			22b. TELEPHONE (Include Area Code) (513) 2553571		22c. OFFICE SYMBOL ENY

UNCLASSIFIED

Aspirating, hot wire concentration probes are used to measure point-wise binary species concentrations in supersonic gaseous flow fields. Calibration of such probes is usually carried out by exposing the probe to a known mixture as it discharges from a fixed volume (or tank.) A new, steady flow method for the calibration of helium/air concentration probes has been developed and has been compared with an existing tank discharge method. The two calibration curves have been found to be in close agreement, with a difference of 0.05 helium molar fraction between them for given a value of wire heat loss. Probe design is suspected of being responsible for this slight variation in helium molar fraction. Hence, either method can be used for calibration of such probes.

UNCLASSIFIED